

EXPERIMENTAL STUDY OF BEAM-INDUCED DAMAGE IN Nb₃Sn SAMPLE COILS PRE-IRRADIATED UP TO 30 MGy*

D. Domange^{†1,3}, D. Gancarzik¹, C. Hernalsteens¹, C. Lannoy¹,
D. Wollmann¹, R. Babouche², M. Bonura², C. Senatore², N. Pauly³

¹CERN, Geneva, Switzerland

²University of Geneva, Geneva, Switzerland

³Université libre de Bruxelles, Brussels, Belgium

Abstract

Superconducting magnets of high-energy accelerators are vulnerable to beam-induced damage and previous experiments have characterized the damage limits of Nb₃Sn sample coils under proton-beam impact. This paper presents a follow-up experiment at CERN's HiRadMat facility investigating the combined effect of radiation ageing and beam impact on superconducting sample coils. The coils were pre-irradiated to simulate the integral dose anticipated for the final-focusing triplet quadrupole magnets of the High Luminosity LHC (HL-LHC) at the end of their lifetime. Following a review of the experimental motivation and preparation of the samples, the final experimental setup is described, including sample positioning and expected temperature profiles under beam impact. Metrology measurements, survey operations, and beam-based alignment, used to ensure adequate beam impact parameters, are detailed together with the proton beam parameters used to irradiate the samples. FLUKA simulations constrained by measured beam size, intensity, and position provide estimates for the local temperature rises and gradients. The timeline of the successfully completed experiment is reviewed. The ongoing post-irradiation analysis, including the assessment of beam-spot characteristics using radiation-sensitive film and the critical-current measurement campaign, is discussed in detail.

INTRODUCTION

The High-Luminosity Large Hadron Collider (HL-LHC) final-focusing triplet quadrupole magnets, the first high-energy accelerator magnets based on Nb₃Sn technology, will be exposed to mixed radiation fields produced at the interaction points of the ATLAS and CMS experiments [1, 2]. Throughout their operational lifetime, they will accumulate a total dose of 20 to 30 MGy, which will degrade the mechanical strength of the CTD101k epoxy impregnating the coils [3–5]. In addition, ultra-fast failure events, such as kicker misfires, can deflect the beam onto an unintended trajectory, generating particle showers that could deposit considerable amounts of energy in the superconducting coils and cause localised heating and mechanical stress [6–12]. The HRMT-61 experiment at the HiRadMat facility of the CERN Super Proton Synchrotron (SPS) characterised the damage limits of non-aged Nb₃Sn racetrack sample coils

under 440 GeV/c proton-beam impact, finding no degradation up to hot-spot temperatures of 670 K and peak strains of 0.5 % [13, 14]. Whether radiation ageing lowers these limits remained unknown. The HRMT-70 experiment was designed to address this question by combining γ -ray pre-irradiation to doses of 25 and 30 MGy with subsequent proton-beam impact at cryogenic temperature [15].

EXPERIMENT DESIGN

The goal of the experiment is to assess the potential impact of radiation ageing on the damage limits by comparing the results to the non-aged results from HRMT-61 [14]. Similar hot-spot temperatures and temperature gradients were therefore targeted for the aged samples, while higher values — above 700 K and 200 K/mm — were sought for non-aged samples to probe the onset of damage. FLUKA [16] simulations were performed to optimise the coil layout and the number of copper shower blocks required. The final plate design is shown in Fig. 1. The most radiation-aged samples (30 MGy) are placed at the lowest hot-spot temperature position, followed by the 25 MGy samples, and finally the non-aged samples (green) at the highest energy deposition positions. There are two batches of four coils with identical spacing and shower-block configuration. One 10 mm thick copper block is placed upstream of the first coil and two additional 9 mm thick blocks are positioned upstream of the last coil of each batch. Simulations were carried out for beam sizes between $\sigma = 1.0$ and 1.3 mm and bunch intensities between 1.2×10^{11} and 1.8×10^{11} protons per bunch (ppb), all of which could be produced at the HiRadMat facility [17, 18].

The optimal parameters — $\sigma = 1.2$ mm and 1.65×10^{11} ppb with 24 bunches — were selected to simultaneously match the four target temperature windows while achieving a gradient above 200 K/mm in the last sample of each batch.

Three complementary systems were integrated into the experimental setup to fully characterise the beam position relative to the samples throughout the experiment. A dedicated beam-based alignment (BBA) window is placed between the two coil batches. It consists of three copper blocks (Fig. 2): two side blocks (W1 and W2), each 9 mm thick and 30 mm tall, forming a horizontal aperture of 16 mm, with one 9 mm thick block (W3) placed on top. The precise dimensions allow the beam centre to be reconstructed relative to the metrology reference frame before the high-intensity shots. Tin foils, to be used for post-irradiation beam-trajectory

* Supported by the HL-LHC project

† delphine.domange@cern.ch

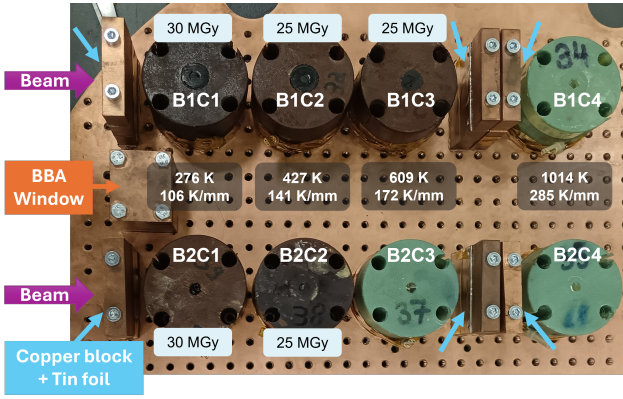


Figure 1: Plate design for the HRMT-70 experiment showing the two batches of four coils (B1 and B2). The beam-based alignment (BBA) window and the tin foils clamped on the copper shower blocks are highlighted.

reconstruction, are fixed to each copper shower block as shown in Fig. 1. The foils are mechanically clamped to the blocks to ensure they remain fixed despite the beam-induced shock waves. Each assembly carries two precision reference holes, enabling post-irradiation beam-trajectory reconstruction from the beam imprint on the foil. Gafchromic EBT3 radiochromic films are placed immediately upstream of each coil and block to provide a two-dimensional image of the beam. Larger films have been placed outside of the vacuum vessel to provide information along the full beam path. Post-irradiation scanning will be used to confirm the beam size and transverse position.

The baseplate is mounted inside a dry cryocooled vacuum vessel (see Fig. 2) maintained at ~ 6 K throughout the experiment, to replicate conditions similar to those encountered during operation [1].

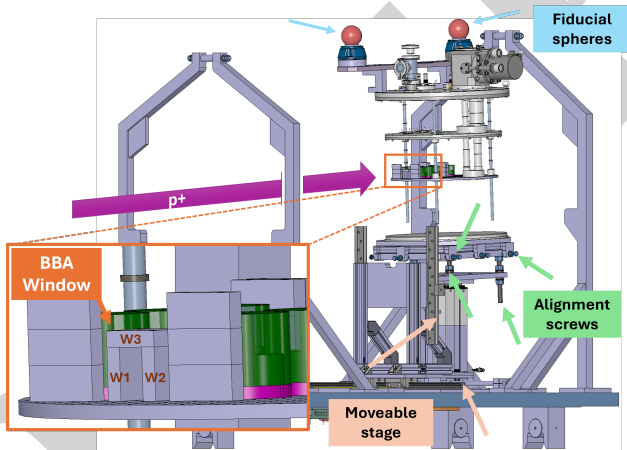


Figure 2: Experimental setup on the HiRadMat table showing the vacuum vessel on the moveable stage relative to the beam. The insulation tanks are removed to show the baseplate position and the BBA window.

PREPARATION AND ALIGNMENT

Metrology and Survey

To precisely determine the coil positions relative to the beam, metrology of the baseplate and the vacuum vessel was performed. A reference frame was established with the y -axis along the foreseen beam direction and the z -origin set 9.6 mm above the plate surface. This corresponds to the winding mid-plane of the coils and served as target height for the beam centre during the impact. The x -origin was placed in the centre of the BBA window. The average horizontal positions of batch 1 and batch 2 coil centres are -50.54 mm and 50.28 mm respectively, with individual coil deviations below 0.21 mm. The average coil height is 46.99 ± 0.16 mm, consistent with the design value of 47 mm. Screw-position measurements gave a screw-to-centre distance of 20.02 ± 0.19 mm (design: 20 mm), confirming the coil geometry, including that of the aged coils whose G10 clamps had been deformed by γ -irradiation.

The BBA window block surfaces were measured. The average positions of the inner (\bar{x}_1 or \bar{z}_1) and outer (\bar{x}_2 or \bar{z}_2) faces are given in Table 1. The tin-foil reference-hole positions and assembly surface coordinates were also measured.

Table 1: BBA window block surface positions from metrology (\bar{x} or \bar{z} : average face position; σ : standard deviation of three measured points).

	\bar{x}_1 (mm)	σ_{x_1}	\bar{x}_2 (mm)	σ_{x_2}
W1	-16.669	0.141	-7.645	0.174
W2	8.250	0.271	17.214	0.228
	\bar{z}_1 (mm)	σ_{z_1}	\bar{z}_2 (mm)	σ_{z_2}
W3	20.278	0.028	29.261	0.031

Five fiducial spheres mounted on the vacuum vessel were measured in the metrology frame and served as reference points for the closed vacuum vessel. Survey operations were conducted in both the surface laboratory and the HiRadMat tunnel, aligning the metrology reference frame to the beam reference frame using alignment screws and motorised horizontal and vertical stages (Fig. 2). After final alignment in the tunnel, the residual horizontal error is -0.05 mm at the beam entrance and -0.003 mm at the exit; the residual vertical error is -0.15 mm and -0.09 mm respectively. Motor scan characterisation revealed a small vertical coupling of -0.39 mm at the B1 position and 0.15 mm at B2. This was considered sufficiently good to justify applying no correction for the high-intensity shots.

Beam-Based Alignment

Despite the metrology and survey, thermal contraction of the assembly at cryogenic temperature introduces positional uncertainties that cannot be corrected a priori. A beam-based alignment (BBA) was therefore performed immediately before the high-intensity shots using single SPS pilot bunches of $\sim 9 \times 10^9$ ppb. Horizontal scans of W1

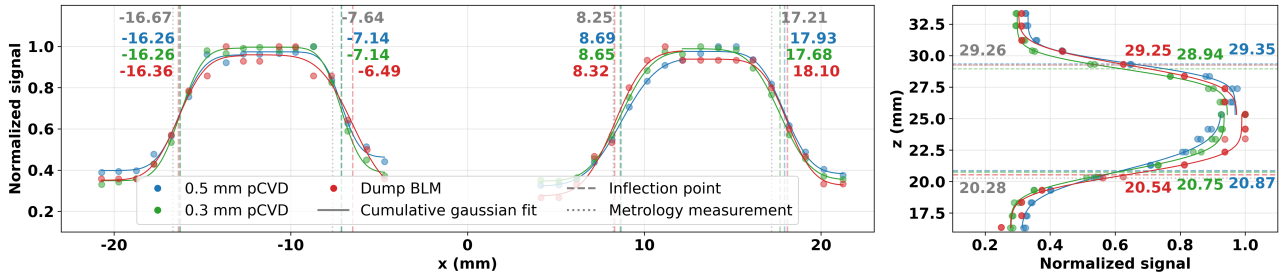


Figure 3: Results of the BBA scan. Each circle corresponds to one pilot bunch. The inflection point of the cumulative Gaussian used to fit the results corresponds to the calculated position of the BBA window edge. For comparison, the results from the metrology measurement of the window surfaces are also represented in gray.

and W2, and a vertical scan of W3, were performed using two pCVD diamond detectors [19] and a BLM on the downstream dump to register the signal produced by the secondary particle shower (Fig. 3). Block edges were extracted by fitting the intensity-normalised signals with a cumulative Gaussian ($R^2 > 0.986$), equivalent to the convolution of the beam profile with a step function. Reconstructed block positions agreed with the metrology values in Table 1 to within ~ 0.4 mm horizontally and ~ 0.5 mm vertically, consistent with the combined uncertainties of metrology, survey, and motor positioning. No correction to the nominal impact position was therefore applied.

BEAM PARAMETERS AND ENERGY DEPOSITION

The HRMT-70 experiment was carried out in October 2025 at the HiRadMat facility. The experimental sequence was comprised of cooling down of the cryogenic vessel to ~ 6 K, BBA scans using pilot bunches, and delivery of two high-intensity pulses — one per batch of superconducting coils. This sequence is reflected in the readings of the temperature sensors located inside the vacuum vessel (Fig. 4). Table 2 summarises the nominal and as-delivered beam parameters for the two shots.

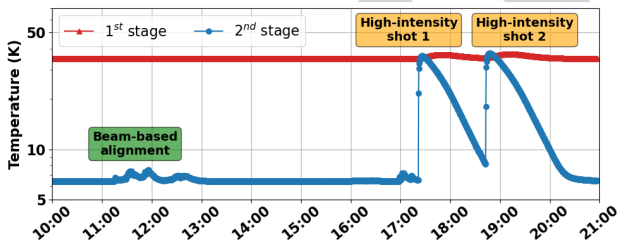


Figure 4: Temperature evolution inside the vacuum vessel during the HRMT-70 experiment. The temperature increase during the BBA scans and the high-intensity shots are clearly visible.

The transverse beam size at the sample location was estimated from measurements by a Beam Television Monitor (BTV) placed at the extraction point, a few metres upstream of the vacuum vessel, and extrapolated to the entrance of the vessel using the proton beam-line optics. A second BTV, located downstream of the vacuum vessel, provided an independent measurement of the beam trajectory, giving the

Table 2: Target and as-delivered beam parameters for the two high-intensity pulses of HRMT-70. The corresponding hot-spot temperature and temperature gradient in the Nb_3Sn sample coils have been computed with FLUKA simulations.

Parameter	Unit	Target	B1	B2
Intensity	(10^{12} p ⁺)	3.96	3.91	3.94
Beam size	σ_x (mm)	1.2	1.18	1.24
	σ_y (mm)	1.2	1.22	1.25
Beam position	x (mm)	0	0.40	0.27
	y (mm)	0	-0.23	-0.22
C1	T (K)	276	276	268
	∇T (K/mm)	106	92	112
C2	T (K)	427	428	416
	∇T (K/mm)	141	139	107
C3	T (K)	609	613	588
	∇T (K/mm)	172	155	185
C4	T (K)	1014	939	947
	∇T (K/mm)	285	261	244

beam position and angle at the entrance of the vacuum vessel. These measured parameters were used as inputs to updated FLUKA simulations to compute the energy deposited in each coil during the experiment; the resulting hot-spot temperatures and temperature gradients are given in Table 2. The Gafchromic film placed across both batches and the BBA window provides a direct visual record of all beam interactions during the experiment, as shown in Fig. 5.

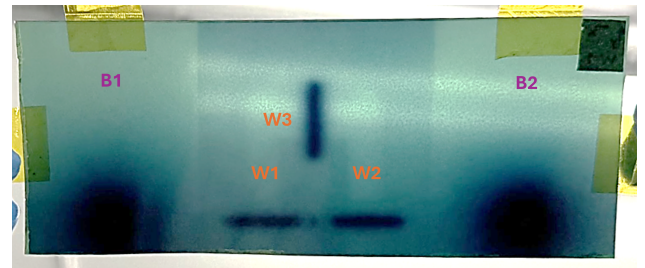


Figure 5: Gafchromic film after the experiment. The central imprint corresponds to the BBA window with the horizontal and vertical scans. The two large dark spots on the left and right correspond to the high-intensity beam impacts on batches B1 and B2 respectively.

CONCLUSION AND OUTLOOK

The HRMT-70 experiment, the first to study the combined effect of radiation ageing and direct beam impact on Nb₃Sn superconducting coils, was successfully completed in October 2025. A rigorous preparation chain — comprising precision metrology of coils, BBA window, tin-foil assemblies, surface and tunnel survey and beam-based alignment — ensured that the beam impacted the coils at the intended positions with well-characterised parameters. FLUKA simulations constrained by the measured beam properties provide the local temperature rises and gradients required to interpret the damage results.

The post-irradiation analysis is ongoing. Gafchromic films and tin-foil imprints are being analysed to refine the beam-position and beam-size reconstruction. Critical-current measurements of the eight irradiated coils at 4.2 K in a 7 T field will be compared to pre-irradiation baselines to quantify any degradation from the combined loading, and to establish whether prior γ -irradiation up to HL-LHC operational dose levels reduces the beam-impact damage limits of Nb₃Sn coils.

ACKNOWLEDGEMENTS

We would like to express our deepest gratitude to all our colleagues from the TE, BE, EN, and SY departments at CERN for their support in preparing and conducting the experiment.

REFERENCES

- [1] G. Apollinari *et al.*, Eds., *High-Luminosity Large Hadron Collider (HL-LHC): Technical Design Report V. 0.1*, CERN, Geneva, Switzerland, Rep. CERN-2017-007-M, 2017. [doi:10.23731/CYRM-2017-004](https://doi.org/10.23731/CYRM-2017-004)
- [2] R. Flükiger, “Irradiation effects in low T_c superconductors”, CERN, Geneva, Switzerland, Rep. CERN-2009-001, 2009. [doi:10.5170/CERN-2009-001.55](https://doi.org/10.5170/CERN-2009-001.55)
- [3] M.-S. Gilarte and F. Cerutti, “Updates of energy deposition studies”, presented at the 13th HL-LHC Collaboration Meeting, Vancouver, Canada, Sep. 2023. <https://indico.cern.ch/event/1293138/contributions/5581018/>
- [4] R. García Alía *et al.*, “LHC and HL-LHC: present and future radiation environment in the high-luminosity collision points and RHA implications”, *IEEE Trans. Nucl. Sci.*, vol. 65, no. 1, pp. 448–456, Jan. 2018. [doi:10.1109/TNS.2017.2776107](https://doi.org/10.1109/TNS.2017.2776107)
- [5] D. M. Parragh *et al.*, “Effect of irradiation temperature and atmosphere on aging of epoxy resins for superconducting magnets”, *Polymers*, vol. 16, no. 3, p. 407, 2024. [doi:10.3390/polym16030407](https://doi.org/10.3390/polym16030407)
- [6] A. Lechner *et al.*, “Protection of superconducting magnets in case of accidental beam losses during HL-LHC injection”, in *Proc. IPAC'15*, Richmond, VA, USA, May 2015, pp. 2128–2131. [doi:10.18429/JACoW-IPAC2015-TUPTY049](https://doi.org/10.18429/JACoW-IPAC2015-TUPTY049)
- [7] J. Uythoven *et al.*, “Injection protection upgrade for the HL-LHC”, in *Proc. IPAC'15*, Richmond, VA, USA, May 2015, pp. 2136–2139. [doi:10.18429/JACoW-IPAC2015-TUPTY051](https://doi.org/10.18429/JACoW-IPAC2015-TUPTY051)
- [8] V. Raginel, “Study of the damage mechanisms and limits of superconducting magnet components due to beam impact”, Ph.D. thesis, TU Vienna, Vienna, Austria, 2018.
- [9] V. Raginel *et al.*, “Change of critical current density in Nb-Ti and Nb₃Sn strands after millisecond heating”, in *Proc. IPAC'17*, Copenhagen, Denmark, May 2017, pp. 3528–3531. [doi:10.18429/JACoW-IPAC2017-WEPVA111](https://doi.org/10.18429/JACoW-IPAC2017-WEPVA111)
- [10] A. Will, “Damage mechanisms in superconductors due to the impact of high energy proton beams and radiation tolerance of cryogenic diodes used in particle accelerator magnet systems”, Ph.D. thesis, Karlsruhe Institut für Technologie, Karlsruhe, Germany, 2021.
- [11] A. Will *et al.*, “Beam impact experiment of 440 GeV/p protons on superconducting wires and tapes in a cryogenic environment”, in *Proc. IPAC'19*, Melbourne, Australia, May 2019, pp. 4264–4267. [doi:10.18429/JACoW-IPAC2019-THPTS066](https://doi.org/10.18429/JACoW-IPAC2019-THPTS066)
- [12] A. Will *et al.*, “Impact of 440 GeV proton beams on superconductors in a cryogenic environment”, *J. Phys.: Conf. Ser.*, vol. 1559, no. 1, p. 012060, 2020. [doi:10.1088/1742-6596/1559/1/012060](https://doi.org/10.1088/1742-6596/1559/1/012060)
- [13] D. Gancarcik *et al.*, “Damage experiment with superconducting sample coils—experimental setup and observations during beam impact”, *J. Phys.: Conf. Ser.*, vol. 2687, no. 8, p. 082014, Jan. 2024. [doi:10.1088/1742-6596/2687/8/082014](https://doi.org/10.1088/1742-6596/2687/8/082014)
- [14] D. Gancarcik *et al.*, “Damage limits of Nb-Ti and Nb₃Sn superconductors due to high-intensity beam impact”, *IEEE Trans. Appl. Supercond.*, vol. 35, no. 7, pp. 1–15, Oct. 2025. [doi:10.1109/TASC.2025.3596324](https://doi.org/10.1109/TASC.2025.3596324)
- [15] D. Gancarcik *et al.*, “Beam impact experiment to qualify the damage limits of Nb₃Sn sample coils pre-irradiated to 30 MGy”, in *Proc. IPAC'25*, Taipei, Taiwan, Jun. 2025, pp. 1807–1810. [doi:10.18429/JACoW-IPAC2025-WEPB034](https://doi.org/10.18429/JACoW-IPAC2025-WEPB034)
- [16] T. T. Böhlen *et al.*, “The FLUKA code: developments and challenges for high energy and medical applications”, *Nucl. Data Sheets*, vol. 120, pp. 211–214, 2014. [doi:10.1016/j.nds.2014.07.049](https://doi.org/10.1016/j.nds.2014.07.049)
- [17] I. Efthymiopoulos *et al.*, “HiRadMat: a new irradiation facility for material testing at CERN”, in *Proc. IPAC'11*, San Sebastian, Spain, Sep. 2011, paper TUPS058, pp. 1665–1667.
- [18] F. Harden *et al.*, “Targetry challenges & HiRadMat”, in *Proc. J-PARC2019*, Ibaraki, Japan, Sep. 2019. [doi:10.7566/JPSCP.33.011149](https://doi.org/10.7566/JPSCP.33.011149)
- [19] Cividec, “B2 poly-crystalline diamond detector”, <https://cividec.at/detectors-B2.html>